

# Mechanisms that direct ordered assembly of T cell receptor $\beta$ locus V, D, and J gene segments

Barry P. Sleckman<sup>\*†</sup>, Craig H. Bassing<sup>\*</sup>, Maureen M. Hughes<sup>†</sup>, Ami Okada<sup>\*\*</sup>, Margaux D'Auteuil<sup>\*</sup>, Tara D. Wehrly<sup>†</sup>, Barbara B. Woodman<sup>\*</sup>, Laurie Davidson<sup>\*</sup>, Jianzhu Chen<sup>\*S</sup>, and Frederick W. Alt<sup>\*†</sup>

<sup>\*</sup>Howard Hughes Medical Institute, Children's Hospital, Harvard Medical School and Center for Blood Research, Boston, MA 02115; and <sup>†</sup>Department of Pathology and Immunology, Washington University School of Medicine, St. Louis, MO 63110

Contributed by Frederick W. Alt, April 27, 2000

T cell receptor (TCR)  $\beta$  variable region genes are assembled in progenitor T cells from germ-line V $\beta$ , D $\beta$ , and J $\beta$  segments via an ordered two-step process in which D $\beta$  to J $\beta$  rearrangements occur on both alleles before appendage of a V $\beta$  to a preexisting DJ $\beta$  complex. Direct joining of V $\beta$  segments to nonrearranged D $\beta$  or J $\beta$  segments, while compatible with known restrictions on the V(D)J recombination mechanism, are infrequent within the endogenous TCR $\beta$  locus. We have analyzed mechanisms that mediate ordered V $\beta$ , D $\beta$ , and J $\beta$  assembly via an approach in which TCR $\beta$  minilocus recombination substrates were introduced into embryonic stem cells and then analyzed for rearrangement in normal thymocytes by recombinase-activating gene 2-deficient blastocyst complementation. These analyses demonstrated that V $\beta$  segments are preferentially targeted for rearrangement to D $\beta$  as opposed to J $\beta$  segments. In addition, we further demonstrated that V $\beta$  segments can be appended to nonrearranged endogenous D $\beta$  segments in which we have eliminated the ability of D $\beta$  segments to join to J $\beta$  segments. Our findings are discussed in the context of the mechanisms that regulate the ordered assembly and utilization of V, D, and J segments.

T cell receptor (TCR) and immunoglobulin (Ig) variable region genes are assembled during progenitor lymphocyte development from variable (V), diversity (D), and joining (J) segments by V(D)J recombination (1, 2). V(D)J recombination is initiated via introduction of DNA double-strand breaks between two participating variable gene segments and their associated recombination signal sequences (RSSs) (3). This reaction is carried out by the lymphocyte-specific recombinase-activating gene 1 (RAG-1) and RAG-2 proteins, which are specifically targeted by the RSSs (4, 5). Subsequently, the cleaved gene segments are joined by a set of generally expressed DNA repair enzymes, which catalyze a nonhomologous end-joining reaction (6). Thus, the specificity of the reaction is provided by the recognition of RSSs by the RAG proteins.

RSSs consist of conserved heptamer and nonamer sequences that flank nonconserved spacers of 12 or 23 bp (hereafter referred to as 12-RSS and 23-RSS, respectively) (1). V(D)J recombination occurs only between gene segments flanked by a 12-RSS and a 23-RSS, a phenomenon referred to as the 12/23 rule (1). This restriction in V(D)J joining is mediated at the level of RAG recognition and cleavage (7, 8). The assembly of all of the different families and types of TCR and Ig variable region gene segments is mediated by the RAG and nonhomologous end-joining proteins, a property based on the relative conservation of the RSSs among the different gene segments. However, despite the relatively generic nature of the basic reaction, V(D)J recombination is tightly regulated in the context of lineage specificity (e.g., TCR variable region genes are assembled in T but not B cells), the context of developmental stage (e.g., TCR $\beta$  variable region genes are assembled before TCR $\alpha$  genes), and in the context of allelic exclusion (9). These observations led to the notion that V(D)J recombination is directed by modulating the

accessibility of the various classes of variable region gene segments to the common V(D)J recombinase (9).

TCR $\beta$  variable region genes are assembled from V $\beta$ , D $\beta$ , and J $\beta$  gene segments in progenitor thymocytes by an ordered process in which D $\beta$  to J $\beta$  rearrangement generally occurs on both alleles before appendage of a V $\beta$  to a preexisting DJ $\beta$  complex. In addition, expression of a TCR $\beta$  protein from a productive V $\beta$ DJ $\beta$  rearrangement prevents V $\beta$  to DJ $\beta$  rearrangement on the second allele and ensures allelic exclusion (10, 11). The mechanisms responsible for ordered assembly of V, D, and J segments or for allelic exclusion of V region gene assembly are not known; however, various considerations suggests that they may be mechanistically linked (12). In this context, the V, D, and J segments of the TCR $\beta$  and IgH loci, which are both assembled in an ordered fashion, also are regulated in the context of allelic exclusion. In contrast, TCR $\delta$  locus V, D, and J segment assembly is not ordered (13), and this locus does not exhibit allelic exclusion (14).

The murine TCR $\beta$  locus is composed of  $\approx 35$  V $\beta$  segments and two D $\beta$ -J $\beta$ -C $\beta$  clusters. V $\beta$  segments are flanked by 3' 23-RSSs and J $\beta$  segments are flanked by 5' 12-RSSs whereas D $\beta$  segments are flanked by 5' 12-RSSs and 3' 23-RSSs (Fig. 1 A and B). Thus, whereas assembly of complete V $\beta$ DJ $\beta$  rearrangements occurs in the context of the 12/23 rule, direct V $\beta$  to J $\beta$  joining is also permissible by the 12/23 rule. Yet, most TCR $\beta$  rearrangements include D $\beta$  nucleotides, suggesting that mechanisms exist to ensure both ordered rearrangement and D $\beta$  segment utilization. The complex organization of the TCR $\beta$  locus presents a challenging obstacle to analyses of mechanisms that direct rearrangement within the locus. To address this issue, we have developed a transgenic TCR $\beta$  minilocus that rearranges in developing T cells and recapitulates many features of the endogenous TCR $\beta$  gene assembly process (15, 16). For example, TCR $\beta$  minilocus rearrangement is ordered, with D $\beta$  to J $\beta$  rearrangement occurring before V $\beta$  to D $\beta$  rearrangement. Moreover, direct V $\beta$  to J $\beta$  rearrangements within the construct appear infrequent, despite the relatively close proximity of these segments in the minilocus (15). Thus, this TCR $\beta$  minilocus should provide an ideal model system to study *cis*-acting elements that regulate ordered TCR $\beta$  gene segment rearrangement.

Abbreviations: TCR, T cell receptor; RAG, recombinase-activating gene; V, variable; D, diversity; J, joining; RDBC, RAG-2-deficient blastocyst complementation; RSS, recombination signal sequence, ES, embryonic stem.

<sup>\*</sup>Present address: Department of Biological Sciences, Stanford University, Stanford, CA 94305.

<sup>S</sup>Center for Cancer Research, Biology Department, Massachusetts Institute of Technology, Cambridge, MA 02139.

<sup>†</sup>To whom reprint requests should be addressed. E-mail: alt@rascal.med.harvard.edu.

The publication costs of this article were defrayed in part by page charge payment. This article must therefore be hereby marked "advertisement" in accordance with 18 U.S.C. §1734 solely to indicate this fact.

Article published online before print: *Proc. Natl. Acad. Sci. USA*, 10.1073/pnas.130190597. Article and publication date are at [www.pnas.org/cgi/doi/10.1073/pnas.130190597](http://www.pnas.org/cgi/doi/10.1073/pnas.130190597)

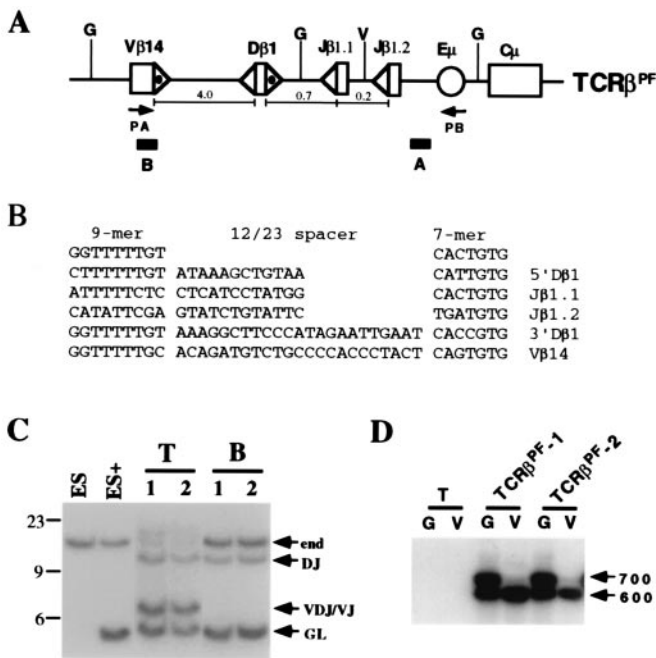


**Fig. 1.** Rearrangement of  $TCR\beta^{PF}$  in T and B cells. (A)  $TCR\beta^{PF}$  contains germ-line  $V\beta 14$ ,  $D\beta 1$ , and  $J\beta 1.1/J\beta 1.2$  gene segments linked to the IgH intronic enhancer ( $E\mu$ ) and constant region gene ( $C\mu$ ). Shown are the locations of probes A and B,  $BglII$  (G) and  $EcoRV$  (V) sites, and the PA and PB oligonucleotide primers. 23-RSSs (dotted  $\Delta$ ) and 12-RSSs ( $\Delta$ ) are indicated. The distances (kb) between gene segments are noted. The minilocus is not drawn to scale. (B) The sequences of the  $V\beta 14$ ,  $D\beta 1$ , and  $J\beta 1.1$  and  $J\beta 1.2$  RSSs are diagrammed below the consensus heptamer and nonamer sequences (29). (C)  $BglII$ -digested genomic DNA subjected to Southern blot analysis by using probe A. DNA was isolated from nontransfected ES cells (ES); ES cells transfected with  $TCR\beta^{PF}$  (ES+); thymocytes (T) and B cells (B) from two independently derived mice,  $TCR\beta^{PF-1}$  (1) and -2 (2), containing the  $TCR\beta^{PF}$  minilocus. Shown are the expected size bands from the nonrearranged endogenous  $TCR\beta$  locus (end) and  $TCR\beta^{PF}$  minilocus (GL). Also shown are the expected size bands from DJ and VDJ/VJ rearrangements of  $TCR\beta^{PF}$ . The 23-, 9-, and 6-kb markers are indicated. (D) PCR analysis was carried out on thymocyte DNA isolated from a non-minilocus-containing wild-type mouse (T) and the  $TCR\beta^{PF-1}$  and -2 mice. Before PCR, genomic DNA was digested with either  $BglII$  (G) or  $EcoRV$  (V).  $EcoRV$  digestion diminishes the amount of VDJ $\beta 1.1$  template. Indicated are the 700- and 600-bp products expected for  $V\beta$  rearrangements to  $J\beta 1.1/DJ\beta 1.1$  and  $J\beta 1.2$ , respectively.

Here we describe two experimental approaches to investigate ordered assembly of  $TCR\beta$  variable region gene segments during T lymphocyte development *in vivo*. First, we assay  $TCR\beta$  minilocus rearrangements in lymphocytes isolated from chimeric mice generated via RAG-2-deficient blastocyst complementation (RDBC) by using embryonic stem (ES) cells into which the minilocus was introduced by transfection (17). This approach permits more rapid *in vivo* analyses than the conventional transgenic method and facilitates analysis of modified constructs. In addition, we have extended such analyses by introducing one of the minilocus alterations into the endogenous chromosomal locus of an ES cell line with a modified endogenous  $TCR\beta$  locus that contains only one D-J $\beta$  cluster (DJ $\beta 1$ ) (18). We have used these approaches to elucidate potential mechanisms that contribute to the ordered rearrangement of  $V\beta$ ,  $D\beta$ , and  $J\beta$  segments.

## Materials and Methods

**$TCR\beta$  Minilocus and Targeting Constructs.** The  $TCR\beta^{PE}$  minilocus was described (ref. 15; referred to as no. 9 transgene). The  $TCR\beta^{PE}$   $BamHI/KpnI$  fragment containing the germ-line  $D\beta 1$ ,  $J\beta 1.1$ , and

$J\beta 1.2$  gene segments was independently subcloned, thereby generating pDJ $\beta$ GL. The M2 mutation was introduced by ligating the annealed oligonucleotides DBAA1GTCTTTTTTGTAT-AAAGCTGTAACATTGTGGGGACAGGGGGCATTTTAA-ATTC and DBAA2-AATTGAATTTAAAATGCCCCCTGTC-CCCACAATGTTACAGCTTTATACAAAAAAG and the  $Eco0109/EcoRI$ -digested 150-bp PCR product generated with primers 5'-CGAATTCTATGGGAAGCCTTTAC-3' and 5'-CCTCTCTCAAGGTCCATCAA-3' into  $Eco0109$ -digested pDJ $\beta$ GL to generate pDJ $\beta$ M2. The  $BamHI/KpnI$  fragment from pDJ $\beta$ M2 was subcloned into  $BamHI/KpnI$ -digested  $TCR\beta^{PF}$  to generate  $TCR\beta^{M2}$ .

The DJ $\beta R^{PF}$  minilocus was constructed by replacing the  $BamHI/KpnI$  fragment of  $TCR\beta^{PF}$  with a fragment containing a DJ $\beta 1.1$  rearrangement (no join diversity) and a germ-line  $J\beta 1.2$  gene segment. To construct DJ $\beta R^C$ , the  $BamHI/KpnI$  fragment from the DJ $\beta R^{PF}$  was independently subcloned, thereby generating p5-1. p5-1 was digested with  $EcoRV$  and  $StuI$  and religated generating p5-1A. PCR product C1 was generated with primers 5'-CGAATTCCAGACTCACAGTTGTAG-3' and 5'-TAT-CAGGACCTACACGGAGGACATGCTTT-3' and product C2 with primers 5'-ACCAAGGTCCCATATTCGAGTATCTGTATT-3' and 5'-TGAATTCCCACACCCAAAGACCC-3'. PCR products C1 and C2 were digested with  $EcoRI$  and  $Eco0109$  and subcloned into  $Eco0109$ -cut p5-1A to generate p5-1B followed by digestion with  $EcoRV$  and  $StuI$  and religation to generate p5-1C. The  $BamHI/KpnI$  fragment from p5-1C was subcloned into  $BamHI/KpnI$ -digested DJ $\beta R^{PF}$  to generate DJ $\beta R^C$ . To construct the DJ $\beta R^D$ , minilocus fragment D1 was generated by PCR amplification of the oligonucleotide 5'-GATCAAGTTCGGGATCCGGGTCCTTTTTTGTAT-AAAGCTGTAACATTGTGCAAACCTCCGACTACACCTTCGGCTCAGGGACCAGGCTTTTGGTAATAGGTAAGATATCCACAG-3' and fragment D2 was generated by PCR amplification of oligonucleotide 5'-GTAGGTAAGATATCTTTCAGGTAATAATTTCCAGGTTCTCTTTCGACAAAGCATGTCTCCGTGTCCATATTCGAGTATCTGTATCTGTATGTGGGACAGGGGGCAAACACAG-AAGTCTTCTTTGGTAAAGGAACCAGACTCACAGTTGTAGGTAAGGCCCTCGAGCCGG-3'. Fragment D1 was digested with  $Eco0109$  and  $EcoRV$  and fragment D2 with  $EcoRV$  and  $StuI$ ; these two fragments were subcloned into  $Eco0109$ - and  $StuI$ -digested p5-1 to generate p5-1D. The  $BamHI/KpnI$  fragment from p5-1D was subcloned into DJ $\beta R^{PF}$  to generate the DJ $\beta R^D$  minilocus.

pM2KI was constructed as described for pM4KI except that the 5' homology region was generated by subcloning the  $Eco0109$  fragment from pDJ $\beta$ M2 into a 2-kb  $NotI/BglII$   $TCR\beta$  genomic DNA fragment (18).

Chimeric mice were generated by RDBC and directly analyzed or bred for germ-line transmission of mutations as described (17, 18).

**Southern and Northern Blot Analyses.** Southern and Northern analyses were carried out as described (19). Probe A is a 300-bp  $EcoRV$  fragment that spans  $J\beta 1.2$  and the downstream region. Probe B is a 600-bp  $AccI$   $V\beta 14$  fragment. Probe C is a 0.8-kb  $DrdI/DrdI$  fragment. Probe D is a 0.4-kb  $BglII/AccI$  fragment. Probe E is a 0.7-kb  $AflIII/HaeII$  fragment. Probe 1 is a 1-kb  $EcoRI$  fragment. Probe 2 is a 2-kb  $HindIII$  fragment. The  $J\beta 1$  probe is a 2-kb  $PstI$  fragment. Glyceraldehyde-3-phosphate dehydrogenase and CD3e cDNA probes have been described (19).

**PCR Analyses.** The oligonucleotide primers used were PA-GGCAAGCAAGCTGGTGTGT, PB-GCATCTCCCTCAAATGAGCC, P1-CCTCTCTCAAGGTCCATCAA, PR1-GCAGAAGAGGATTTCCCTGC, and  $V\beta 14$ -GGCAAGCAAGCTGGTGTGT. The PV  $V\beta$  primer set has been de-

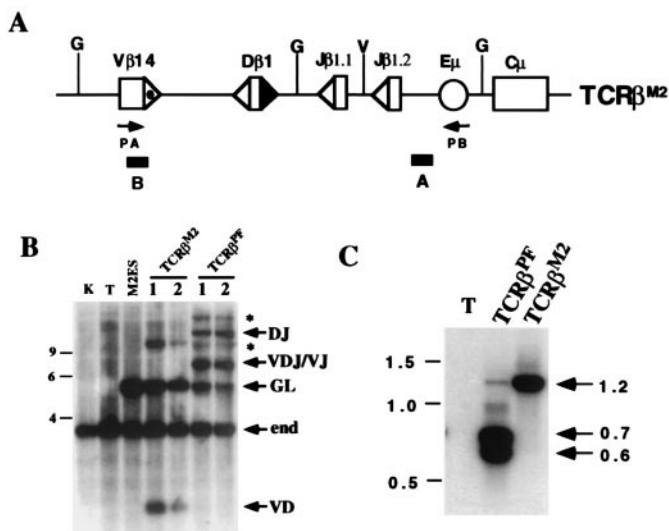


**Fig. 2.** Analysis of  $TCR\beta^{M2}$  rearrangement in T cells. (A)  $TCR\beta^{M2}$  is similar to  $TCR\beta^{PF}$  (Fig. 1A) except for mutation of the 3'  $D\beta 1$  23-RSS heptamer ( $\blacktriangle$ ) as described in the text. The remaining 23-RSS (dotted  $\triangle$ ) and 12-RSSs ( $\triangle$ ) are indicated. (B) *Bgl*II-digested genomic DNA isolated from kidney (K), thymocytes (T), ES cells transfected with  $TCR\beta^{M2}$  (M2ES), or thymocytes isolated from mice containing  $TCR\beta^{M2}$  or  $TCR\beta^{PF}$  miniloci was subjected to Southern blot analysis by using probe B. Shown are the expected size bands from the nonrearranged endogenous  $TCR\beta$  locus (end), and the  $TCR\beta^{M2}$  and  $TCR\beta^{PF}$  miniloci in the nonrearranged (GL), DJ, V(D)J/VJ, and VD rearrangement configurations. Also indicated (\*) are the bands representing pseudonormal joins between tandemly integrated copies of the miniloci which have been described (15). The 9-, 6-, and 4-kb markers are shown. (C) PCR was carried out with primers PA and PB on thymocyte DNA from a wild-type (T),  $TCR\beta^{PF}$ , and  $TCR\beta^{M2}$  mice. Indicated are the 1.2-, 0.7-, and 0.6-kb products expected for V $\beta$  rearrangements to  $D\beta 1$ , (D)J $\beta 1.1$ , and (D)J $\beta 1.2$ , respectively. The 1.5-, 1.0-, and 0.5-kb markers are shown.

scribed (20). PCR conditions were as described with the following cycle conditions: 92°C for 90 s; 60°C for 150 s; 72°C for 60 s for 30 cycles (20).

**Flow Cytometry.** Single-cell suspensions were prepared from thymus and spleen as described (19). Cells were stained with FITC-conjugated anti-CD8 and phycoerythrin-conjugated anti-CD4 antibodies (PharMingen) and analyzed by a FACScan (Becton Dickinson).

## Results

**Efficient Lineage-Specific Recombination of the  $TCR\beta$  Minilocus in Chimeric Mice Generated by RDBC.** We have described a transgenic  $TCR\beta$  minilocus (hereafter referred to as  $TCR\beta^{PF}$ ) that contains germ-line V $\beta 14$ ,  $D\beta 1$ , J $\beta 1.1$ , and J $\beta 1.2$  gene segments linked to the IgH  $\mu$  constant region ( $C\mu$ ) gene (Fig. 1A) (15, 16). In transgenic mice, this minilocus undergoes enhancer-dependent  $D\beta$  to J $\beta$  rearrangement in B and T cells, with V $\beta$  to DJ $\beta$  rearrangement occurring only in T cells (Fig. 1C) (15, 16). Furthermore, minilocus  $D\beta$  to J $\beta$  rearrangement generally precedes V $\beta$  to  $D\beta$  rearrangement (Fig. 2B) (15). To facilitate this approach, we used cotransfection with a PGK-Neor<sup>r</sup>-selectable marker gene to generate ES cell lines with low copy numbers of  $TCR\beta^{PF}$  (Fig. 1C; compare ES to ES+ lanes). These transfected ES cells were used to generate chimeric mice by RDBC; in these mice, the vast majority of thymocytes and all peripheral T cells derive from the transfected ES cells (17).

Southern blot analyses of genomic DNA isolated from thymocytes and purified peripheral B cells revealed  $TCR\beta^{PF}$   $D\beta$  to J $\beta$  rearrangement in B and T cells, with V $\beta$  to DJ $\beta$  rearrange-

ments occurring only in T cells (Fig. 1C). PCR analyses of thymocyte DNA demonstrated that efficient V $\beta$ (D)J $\beta$  rearrangement occurred to both J $\beta 1.1$  and J $\beta 1.2$  gene segments (Fig. 1D). In addition, V $\beta$  to  $D\beta$  rearrangement within  $TCR\beta^{PF}$  was not detectable by Southern blotting, although low levels were detectable by PCR (Fig. 2B and C). Together, these data demonstrate that the  $TCR\beta^{PF}$  minilocus undergoes efficient lineage-specific recombination that recapitulates many aspects of endogenous  $TCR\beta$  rearrangement when transfected into ES cells and assayed for rearrangement in T lineage cells generated by RDBC. In addition, these studies show that germ-line passage of the  $TCR\beta^{PF}$  minilocus is not required to set up normal regulatory constraints and that such constraints are not markedly influenced by the cotransfected PGK-Neor<sup>r</sup> cassette.

**DJ $\beta$  Assembly Is Not Required for V $\beta$  Rearrangement.** To determine whether V $\beta$  segments must rearrange to an assembled DJ $\beta$ , a version of  $TCR\beta^{PF}$  ( $TCR\beta^{M2}$ ) was generated in which the 3'  $D\beta 1$  RSS heptamer (CACAGTG) was replaced with an irrelevant sequence (ATTTTAA) and assayed by RDBC (Fig. 2A). As predicted, the  $TCR\beta^{M2}$  minilocus failed to undergo  $D\beta$  to J $\beta$  rearrangement (Fig. 2B). However, V $\beta$  to  $D\beta$  rearrangement within  $TCR\beta^{M2}$ , in contrast to  $TCR\beta^{PF}$ , was readily detectable by Southern blotting, as well as by PCR (Fig. 2B and C). Together, these data demonstrate that DJ $\beta$  rearrangement *per se* is not required for V $\beta$  to  $D\beta$  rearrangement within the minilocus. Furthermore, direct V $\beta$  to J $\beta$  rearrangements within  $TCR\beta^{M2}$  were not observed, despite 12/23 compatibility of the V $\beta$  23-RSS and the J $\beta$  12-RSSs (Fig. 2B).

To investigate whether the rearrangement patterns observed in the  $TCR\beta$  minilocus accurately reflected those of the endogenous  $TCR\beta$  locus, gene targeting was used to introduce the M2 mutation into a single  $TCR\beta$  allele (J $\beta 1^{M2}$ ) of the J $\beta 1^{\omega/\omega}$  ES cell line (Fig. 3A). The DJ $\beta 2$  gene cluster was deleted by gene targeting and replaced by single *loxP* sites on both  $TCR\beta$  alleles of the J $\beta 1^{\omega/\omega}$  ES line (Fig. 3A) (18). J $\beta 1^{\omega/\omega}$  mice exhibit normal T cell development with  $TCR\beta$  rearrangements limited to the DJ $\beta 1$  gene cluster (18). J $\beta 1^{M2/\omega}$  ES cells were used to generate chimeric mice by RDBC that were analyzed directly or bred for germ-line transmission of the mutant J $\beta 1^{M2}$  allele. Flow cytometric analyses revealed that T cell development proceeded normally in J $\beta 1^{M2/\omega}$  mice (data not shown). Southern blot analysis of J $\beta 1^{M2/\omega}$   $\alpha\beta$  T cell hybridomas showed that all had J $\beta 1$  rearrangements on the J $\beta 1^{\omega}$  allele, whereas only one had undergone a J $\beta 1$  rearrangement on the J $\beta 1^{M2}$  allele (Table 1). Of these hybridomas, 22 (21%) had undergone a V $\beta$  to  $D\beta 1$  rearrangement on the J $\beta 1^{M2}$  allele (Table 1). Furthermore, these V $\beta$  to  $D\beta 1$  rearrangements used a diverse V $\beta$  repertoire (Fig. 3B). Together, these data demonstrate that  $D\beta$  to J $\beta$  rearrangement of either the minilocus or the endogenous  $TCR\beta$  locus is not required for rearrangement of a diverse set of V $\beta$  segments to a previously nonrearranged  $D\beta$  segment. In addition, these findings further confirm that the  $TCR\beta$  minilocus accurately recapitulates rearrangement patterns of the endogenous  $TCR\beta$  locus.

Despite 12/23 compatibility between V $\beta$  23-RSSs and J $\beta$  12-RSSs, only one of the 106 J $\beta 1^{M2/\omega}$  splenic  $\alpha\beta$  T cell hybridomas had undergone a V $\beta$  to J $\beta 1$  rearrangement on the J $\beta 1^{M2}$  allele (Table 1). Consistent with this, J $\beta 1^{M2/M2}$  mice exhibited a significant block in thymocyte development at the CD4<sup>-</sup>/CD8<sup>-</sup> (double negative) stage (Fig. 3C) and reduced numbers of mature splenic T cells (data not shown). Failure of V $\beta$  to J $\beta$  joining on the J $\beta 1^{M2}$  allele was not caused by diminished germ-line J $\beta$  transcripts as evidenced by the equivalent levels of these transcripts in double-negative thymocytes isolated from RAG-2<sup>-/-</sup> and RAG-2<sup>-/-</sup>:J $\beta 1^{M2/M2}$  mice (Fig. 3D). Together, these data demonstrate that there is a significant bias for V $\beta$  to

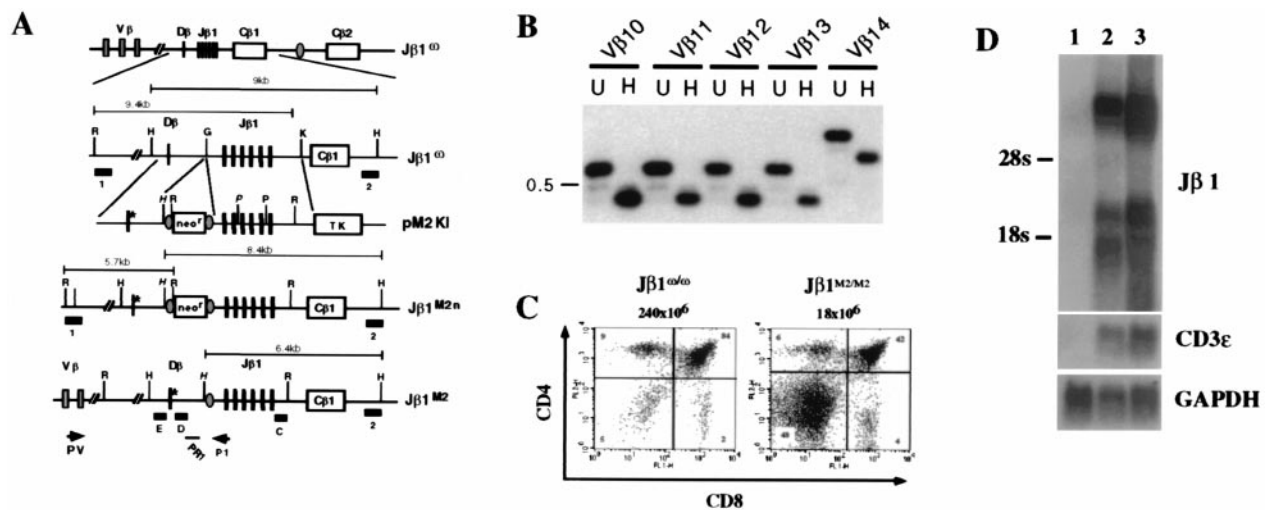


**Fig. 3.** Generation and analysis of mice with M2 mutation in the endogenous TCR $\beta$  locus. (A) Schematic of the  $J\beta 1^{\omega}$  allele showing some of the  $V\beta$  gene segments, the  $DJ\beta 1$  gene cluster, the  $loxP$  site (shaded oval) that replaces the  $DJ\beta 2$  gene cluster, and the  $C\beta 1$  and  $C\beta 2$  genes (not to scale).  $J\beta 1^{\omega/\omega}$  ES cells were transfected with the pM2KI targeting vector to generate the  $J\beta 1^{M2/\omega}$  allele. Cre-mediated deletion of the  $loxP$ -flanked  $neo^+$  gene generates the  $J\beta 1^{M2}$  allele which differs from the  $J\beta 1^{\omega}$  allele by the presence of the M2 mutant heptamer (\*), an introduced  $HindIII$  site ( $H$ ), and a single  $loxP$  site that is not contiguous with the mutation. Shown are  $EcoRI$  ( $R$ ),  $HindIII$  ( $H$ ), and  $KpnI$  ( $K$ ) sites. The position of probes 1, 2, C, D, and E are shown as filled rectangles. Probes 1 and 2 were used to identify correctly targeted alleles (data not shown). Also shown is the position of oligonucleotide primer P1 and probe PR1. PV is a described (20) set of  $V\beta$  gene segment primers. (B) PCR analyses of  $J\beta 1^{M2/\omega}$  thymocyte DNA by using the PV panel of  $V\beta$  primers and the P1 primer. Shown are PCR reactions by using  $V\beta 10$ - to  $V\beta 14$ -specific primers with the P1 primer. Southern blot analysis of undigested (U) or  $HindIII$ -digested (H) PCR products was carried out by using the PR1 oligonucleotide probe. PCR products from  $V\beta$  to  $D\beta$  rearrangements on the  $J\beta 1^{M2}$  allele are reduced in size on  $HindIII$  digestion. The 0.5-kb marker is indicated. (C) Flow cytometric analysis of thymocytes from 3- to 4-week-old  $J\beta 1^{\omega/\omega}$  and  $J\beta 1^{M2/M2}$  mice by using CD4-PE and CD8-FITC. Shown is a representative analysis of the eight  $J\beta 1^{\omega/\omega}$  and  $J\beta 1^{M2/M2}$  mice analyzed. (D) Whole-cell RNA was isolated from RAG-2 $^{-/-}$  spleen (lane 1), RAG-2 $^{-/-}$  thymus (lane 2), and  $J\beta 1^{M2/M2};RAG-2^{-/-}$  thymus (lane 3) and subjected to Northern blot analysis by using a probe that spans the  $J\beta 1$  gene segments ( $J\beta 1$ ) and the CD3 $\epsilon$  and glyceraldehyde-3-phosphate dehydrogenase probes as controls.

$D\beta$  versus  $V\beta$  to  $J\beta$  rearrangement despite the 12/23 compatibility of both steps.

**Efficient TCR $\beta$  Minilocus  $V\beta$  Rearrangement to a Preassembled  $DJ\beta$  Complex.** To elucidate cis-acting elements that promote preferential rearrangement of  $V\beta$  segments to  $D\beta$  versus  $J\beta$  segments, we conducted a systematic mutational analysis of the TCR $\beta^{PF}$  minilocus. First, we constructed a modified TCR $\beta^{PF}$  construct ( $DJ\beta R^{PF}$ ) in which the germ-line  $D\beta 1$  and  $J\beta 1.1$  gene segments were replaced with a  $DJ\beta 1.1$  rearrangement (Fig. 4A). As assayed by RDBC and Southern blot analysis of thymocyte and B cell genomic DNA,  $DJ\beta R^{PF}$  showed efficient  $V\beta$  to  $DJ\beta$  rearrangement in T but not B lymphocytes (Fig. 4B). PCR analyses of  $DJ\beta R^{PF}$  revealed that  $V\beta$  rearrangement occurred exclusively to  $DJ\beta 1.1$  (Fig. 4C), despite the observation that the  $J\beta 1.2$  gene segment is competent for rearrangement as indicated by efficient TCR $\beta^{PF}$   $D\beta$  to  $J\beta 1.2$  rearrangement (Fig. 1D) (15, 16, 21, 22). Consequently, the  $DJ\beta R^{PF}$  minilocus, like the endogenous TCR $\beta$  locus, exhibits a significant bias for  $V\beta$  to  $D\beta$  versus  $V\beta$  to  $J\beta$  rearrangement.

**Table 1. Analysis of TCR $\beta$  rearrangements in  $J\beta 1^{\omega/\omega}$  and  $J\beta 1^{M2/\omega}$   $\alpha\beta$  T cell hybridomas**

Hybridoma	Total no.	Allele	No. with rearrangements			
			GL	DJ	VD	V(D)J
$J\beta 1^{\omega/\omega}$	50	$\omega$	0	34	0	16
		$\omega$	0	0	0	50
$J\beta 1^{M2/\omega}$	106	$\omega$	0	1	0	105
		M2	83	0	22	1

TCR $\beta$  allele configuration in T cell hybridomas was determined by Southern blot analysis of  $HindIII$ - or  $EcoRI$ -digested genomic DNA by using probes C, D, and E (Fig. 3A). GL, nonrearranged.

**TCR $\beta$   $V\beta$  to  $DJ\beta$  Rearrangement Bias Is Not Positional or Coding Sequence Dependent.** The bias for  $V\beta$  to  $D\beta$  versus  $V\beta$  to  $J\beta$  rearrangement could be enforced by the relative position of the  $D\beta$  and  $J\beta$  gene segments, with  $V\beta$  rearrangement targeted to the most proximal 12-RSS. To test this notion, we constructed a modified  $DJ\beta R^{PF}$  minilocus,  $DJ\beta R^C$ , in which the position of the  $DJ\beta 1.1$  and  $J\beta 1.2$  coding sequences and their associated 12-RSSs were exchanged (Fig. 4A). Southern blot analysis revealed that  $DJ\beta R^C$  undergoes efficient rearrangement in thymocytes (data not shown). Moreover, PCR analyses of thymocyte DNA revealed significant  $DJ\beta R^C$   $V\beta$  to  $DJ\beta 1.1$  rearrangement with no readily detectable  $V\beta$  to  $J\beta 1.2$  rearrangement (Fig. 4C). Therefore, the bias for  $V\beta$  to  $DJ\beta$  rearrangement is not specified to the most proximal 5'12-RSS, but is rather targeted specifically to the  $D\beta$  versus the  $J\beta$  elements.

Recombination substrate studies have shown that V(D)J recombination efficiency can be influenced by coding sequences (23–27). To address this possibility, we constructed a modified  $DJ\beta R^{PF}$  minilocus,  $DJ\beta R^D$ , in which the  $DJ\beta 1.1$  and  $J\beta 1.2$  coding sequences were exchanged, but the native positions of their associated 5' RSSs were maintained (Fig. 4A). After RDBC, Southern blot analysis of thymocyte DNA again confirmed that  $DJ\beta R^D$  undergoes efficient rearrangement in thymocytes (data not shown). Significantly, however, PCR analyses of  $DJ\beta R^D$  revealed  $V\beta$  to  $J\beta 1.2$  rearrangement with no detectable  $V\beta$  to  $DJ\beta 1.1$  rearrangement (Fig. 4C). This finding shows that the bias in  $V\beta$  to  $DJ\beta 1.1$  rearrangement is not determined by  $D\beta$  coding sequences, and therefore, most likely is specified by the  $D\beta$  versus  $J\beta$  5'12-RSS sequences.

## Discussion

**Restraints Beyond 12/23 Compatibility Restrict Joining of  $V\beta$  to  $D\beta$  Versus  $J\beta$  Segments.** Direct  $V\beta$  to  $J\beta$  rearrangement satisfies the 12/23 rule. However, our analyses of the M2 mutation clearly

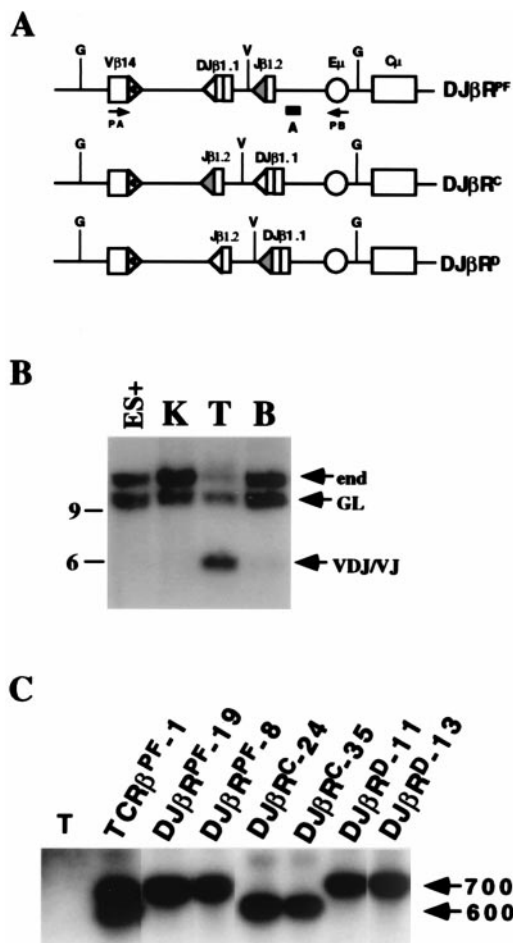


**Fig. 4.** Analysis of DJ $\beta$ R<sup>PF</sup>, DJ $\beta$ R<sup>C</sup>, and DJ $\beta$ R<sup>D</sup> rearrangement in T cells. (A) Schematic of DJ $\beta$ R<sup>PF</sup>, DJ $\beta$ R<sup>C</sup>, and DJ $\beta$ R<sup>D</sup> miniloci. In DJ $\beta$ R<sup>PF</sup>, the germ-line D $\beta$ 1/J $\beta$ 1.1 gene segments and intervening sequence of TCR $\beta$ <sup>PF</sup> has been replaced by a preassembled DJ $\beta$ 1.1 rearrangement. In DJ $\beta$ R<sup>C</sup>, the position of DJ $\beta$ 1.1 and J $\beta$ 1.2 and their flanking RSSs have been exchanged. In DJ $\beta$ R<sup>D</sup>, the position of the coding region of DJ $\beta$ 1.1 and J $\beta$ 1.2 has been exchanged with the RSSs remaining in their native positions. The J $\beta$ 1.2 12-RSS (shaded triangle), D $\beta$ 1 12-RSS (open triangle), and V $\beta$ 14 23-RSS (dotted open triangle) are indicated. (B) BglII-digested genomic DNA isolated from kidney (K) and ES cells transfected with DJ $\beta$ R<sup>PF</sup> or thymocytes (T) and B cells (B) from a mouse with the DJ $\beta$ R<sup>PF</sup> minilocus was subjected to Southern blot analysis by using probe A (Fig. 1). Shown are the expected size bands from the nonrearranged endogenous TCR $\beta$  locus (end) and nonrearranged (GL) or VDJ/VJ-rearranged DJ $\beta$ R<sup>PF</sup> minilocus. The 9- and 6-kb markers are indicated. (C) The PA and PB primers were used to PCR thymocyte DNA from wild-type non-miniloci-containing mice (T) or mice that have the TCR $\beta$ <sup>PF</sup> (-1), DJ $\beta$ R<sup>PF</sup> (-8, -19), DJ $\beta$ R<sup>C</sup> (-24, -35), or DJ $\beta$ R<sup>D</sup> (-11, -13) miniloci. Analyses shown are from mice generated from independently derived ES cells. Genomic DNA was digested with BglII before PCR; PCR products were subjected to Southern blot analysis by using probe A. V $\beta$  rearrangement to the J $\beta$ 1.2 RSS (shaded triangle) yields a 700-bp PCR product from DJ $\beta$ R<sup>C</sup> and 600-bp PCR products from DJ $\beta$ R<sup>PF</sup> and DJ $\beta$ R<sup>D</sup>.

revealed a substantial bias for V $\beta$  to D $\beta$  versus V $\beta$  to J $\beta$  rearrangement, despite 12/23 compatibility of the V $\beta$  and J $\beta$  RSSs. To further elucidate elements responsible for this bias, we analyzed a modified version of the TCR $\beta$ <sup>PF</sup> minilocus with a preassembled DJ $\beta$ 1.1 and germ-line J $\beta$ 1.2 gene segments (DJ $\beta$ R<sup>PF</sup>). These studies showed preferential V $\beta$  to D $\beta$  rearrangement when the DJ $\beta$ 1.1 complex is positioned downstream of J $\beta$ 1.2, demonstrating that the bias is not imparted by relative proximity of D $\beta$  and J $\beta$  segments to V $\beta$ . In addition, we observed specific V $\beta$  targeting to the J $\beta$ 1.2 coding sequence

when this coding sequence was adjacent to the 5'D $\beta$  12-RSS (DJ $\beta$ R<sup>C</sup>), whereas rearrangement was not observed to the D $\beta$  coding sequence when it was flanked by the J $\beta$ 1.2 12-RSS (DJ $\beta$ R<sup>D</sup>). Taken together, these findings reveal that unanticipated regulatory constraints, independent of simple positional effects or the 12/23 rule, target V $\beta$  rearrangement to D $\beta$  segments and prevent efficient V $\beta$  to J $\beta$  rearrangement.

Our mutational analyses strongly suggest that this novel constraint in the V(D)J recombination reaction is determined by distinct features of the 5'D $\beta$ 1 and J $\beta$ 1 12-RSSs beyond simply enforcing the 12/23 rule. In parallel studies, we tested whether these conclusions apply to endogenous loci by generating and analyzing mice with appropriate mutations in the J $\beta$ 1 <sup>$\omega$</sup>  TCR $\beta$  allele (18). These studies clearly confirmed that the 5' D $\beta$ 1 12-RSS, and not the J $\beta$  12-RSSs, specifically and precisely targets V $\beta$  rearrangement (18). Whereas the mechanism responsible for this phenomenon remains to be fully elucidated, the observed rearrangement bias clearly results from RSS sequence constraints beyond 12/23 compatibility. Such constraints may have important implications for V $\beta$  repertoire development and potentially for enforcing allelic exclusion at the V $\beta$  to D $\beta$  step (18). Finally, we note that our studies show that direct V $\beta$  to J $\beta$  joining can occur at low frequency in J $\beta$ 1<sup>M2/M2</sup> mice and lead to the generation of T cells. Given that the productive TCR $\beta$  rearrangements generated from direct V $\beta$ J $\beta$  joins use a large repertoire of different V $\beta$  gene segments, most or all V $\beta$  segments appear to retain a similarly inefficient ability to be joined directly to a J $\beta$  segment.

**Factors That Effect Ordered Rearrangement of TCR $\beta$  V, D, and J Segments.** Endogenous TCR $\beta$  V region gene assembly is ordered with D $\beta$  to J $\beta$  rearrangements occurring on both alleles before V $\beta$  appendage to a DJ $\beta$  complex. Yet, V $\beta$  to D $\beta$  rearrangement occurred quite readily in the TCR $\beta$ <sup>M2</sup> minilocus that lacked a functional 3' D $\beta$  23-RSS (M2 mutation) and which is, thus, incapable of D $\beta$  to J $\beta$  rearrangement. It seemed possible that this unanticipated observation may not apply to the endogenous locus, in which much greater distances and other sequences separate the rearranging elements. To address this issue, we introduced the M2 mutation into an ES cell line with a modified TCR $\beta$  locus (J $\beta$ 1 <sup>$\omega$</sup> ) that contains only the D-J $\beta$ 1 gene cluster (18). Consistent with the TCR $\beta$ <sup>M2</sup> minilocus results, significant levels of V $\beta$  to D $\beta$  rearrangements, but few V $\beta$  to J $\beta$  rearrangements, occurred in the absence of D $\beta$  to J $\beta$  rearrangement within the endogenous TCR $\beta$  locus.

Ordered rearrangement was first described in the IgH locus (D<sub>H</sub> to J<sub>H</sub> before V<sub>H</sub> appendage to DJ<sub>H</sub>) and proposed to be important for regulation of IgH V region gene assembly in the context of allelic exclusion (12). Similar conclusions were reached regarding the TCR $\beta$  V region gene locus (10). In the IgH locus, the V<sub>H</sub> and J<sub>H</sub> segments have 23-RSSs, whereas the D<sub>H</sub> segments have 5' and 3' 12-RSSs. Therefore, direct joining of V<sub>H</sub> to J<sub>H</sub> segments would be prohibited by the 12/23 rule. However, whereas the RSS structure of the IgH locus prescribes D<sub>H</sub> to J<sub>H</sub> and V<sub>H</sub> to D<sub>H</sub> joining, it does not prescribe an order for these events. The novel constraints imposed by RSSs that we observed in the TCR $\beta$  minilocus also enforce D $\beta$  to J $\beta$  and V $\beta$  to D $\beta$  joining, but in a fashion that goes beyond the 12/23 rule. However, as was the case for the IgH locus, these constraints again would not prescribe a precise order.

Our studies of the M2 mutation provide additional insight into ordered rearrangement by showing that D $\beta$  to J $\beta$  rearrangement *per se* is not a prerequisite for V $\beta$  appendage to a D $\beta$ . In addition, this process does not require deletion of sequences between the 3' D $\beta$  23-RSS and J $\beta$  or formation of a DJ $\beta$  complex. Therefore, our finding that direct V $\beta$  to D $\beta$  joins are readily detected in normal thymocytes that harbor the M2 allele suggests other

testable possibilities. One would be that  $D\beta$  to  $J\beta$  rearrangement would enhance  $V\beta$  rearrangement to the 5'D $\beta$  12-RSS by removal of the 3'D $\beta$  23-RSS that could theoretically be a higher affinity site for RAG interaction. Another, based on prior observations, would be that  $D\beta$  to  $J\beta$  rearrangement occurs at an earlier developmental stage than  $V\beta$  rearrangements, but that progenitor T cells can transit to the  $V\beta$ -rearranging stage (perhaps at reduced frequency) without generating a  $DJ\beta$  rearrangement (28). In either case, our overall findings, including the 12/23 restriction, raise the intriguing possibility that

productive TCR $\beta$  rearrangement could mediate allelic exclusion through the generation of a signal that modulates recombinase access to the 5'  $D\beta$  12-RSSs.

This work was supported in part by the National Institutes of Health Grants AI01297 (B.P.S.) and AI20047 (F.W.A.). B.P.S. is a recipient of a Career Development Award from the Burroughs Wellcome Fund. C.H.B. was a fellow of the Irvington Institute for Immunological Research. F.W.A. is an Investigator of the Howard Hughes Medical Institute.

1. Tonegawa, S. (1983) *Nature (London)* **302**, 575–581.
2. Blackwell, T. K. & Alt, F. W. (1989) *Annu. Rev. Genet.* **23**, 605–636.
3. Gellert, M. (1997) *Adv. Immunol.* **64**, 39–64.
4. Schatz, D. G., Oettinger, M. A. & Schlissel, M. S. (1992) *Annu. Rev. Immunol.* **10**, 359–383.
5. McBlane, J. F., van Gent, D. C., Ramsden, D. A., Romeo, C., Cuomo, C. A., Gellert, M. & Oettinger, M. A. (1995) *Cell* **83**, 387–395.
6. Weaver, D. T. (1995) *Adv. Immunol.* **58**, 29–85.
7. Eastman, Q. M., Leu, T. M. & Schatz, D. G. (1996) *Nature (London)* **380**, 85–88.
8. van Gent, D. C., McBlane, J. F., Ramsden, D. A., Sadofsky, M. J., Hesse, J. E. & Gellert, M. (1995) *Cell* **81**, 925–934.
9. Sleckman, B. P., Gorman, J. R. & Alt, F. W. (1996) *Annu. Rev. Immunol.* **14**, 459–481.
10. Uematsu, Y., Ryser, S., Dembic, Z., Borgulya, P., Krimpenfort, P., Berns, A., von Boehmer, H. & Steinmetz, M. (1988) *Cell* **52**, 831–841.
11. Malissen, M., Trucy, J., Jouvin-Marche, E., Cazenave, P. A., Scollay, R. & Malissen, B. (1992) *Immunol. Today* **13**, 315–322.
12. Alt, F. W., Yancopoulos, G. D., Blackwell, T. K., Wood, C., Thomas, E., Boss, M., Coffman, R., Rosenberg, N., Tonegawa, S. & Baltimore, D. (1984) *EMBO J.* **3**, 1209–1219.
13. Krangel, M. S., Hernandez-Munain, C., Lauzurica, P., McMurry, M., Roberts, J. L. & Zhong, X.-P. (1998) *Immunol. Rev.* **165**, 131–147.
14. Sleckman, B. P., Khor, B., Monroe, R. & Alt, F. W. (1998) *J. Exp. Med.* **188**, 1465–1471.
15. Ferrier, P., Krippel, B., Blackwell, T. K., Furley, A. J., Suh, H., Winoto, A., Cook, W. D., Hood, L., Costantini, F. & Alt, F. W. (1990) *EMBO J.* **9**, 117–125.
16. Okada, A., Mendelsohn, M. & Alt, F. W. (1994) *J. Exp. Med.* **180**, 261–272.
17. Chen, J., Lansford, R., Stewart, V., Young, F. & Alt, F. W. (1993) *Proc. Natl. Acad. Sci. USA* **90**, 4528–4532.
18. Bassing, C. H., Alt, F. W., Hughes, M. H., D'Auteuil, M., Wehrly, T., Woodman, B. B., Gartner, F., White, M., Davidson, L. & Sleckman, B. P. (2000) *Nature (London)* **405**, 583–586.
19. Sleckman, B. P., Bardoni, C. G., Ferrini, R., Davidson, L. & Alt, F. W. (1997) *Immunity* **7**, 505–515.
20. Gartner, F., Alt, F. W., Monroe, R., Chu, M., Sleckman, B. P., Davidson, L. & Swat, W. (1999) *Immunity* **10**, 537–546.
21. Ferrier, P., Covey, L. R., Suh, H., Winoto, A., Hood, L. & Alt, F. W. (1989) *Int. Immunol.* **1**, 66–74.
22. Demengeot, J., Oltz, E. M. & Alt, F. W. (1995) *Int. Immunol.* **7**, 1995–2003.
23. Boubnov, N. V., Wills, Z. P. & Weaver, D. T. (1995) *Nucleic Acids Res.* **23**, 1060–1067.
24. Gerstein, R. M. & Lieber, M. R. (1993) *Genes Dev.* **7**, 1459–1469.
25. Nadel, B. & Feeney, A. J. (1995) *J. Immunol.* **155**, 4322–4329.
26. Ezekiel, U. R., Engler, P., Stern, D. & Storb, U. (1995) *Immunity* **2**, 381–389.
27. VanDyk, L. F., Wise, T. W., Moore, B. B. & Meek, K. (1996) *J. Immunol.* **157**, 4005–4015.
28. Livak, F., Tourigny, M., Schatz, D. G. & Petrie, H. T. (1999) *J. Immunol.* **162**, 2575–2580.
29. Hesse, J. E., Lieber, M. R., Mizuuchi, K. & Gellert, M. (1989) *Genes Dev.* **3**, 1053–1061.